e-PS, 2012, **9**, 47-59
ISSN: 1581-9280 web edition
ISSN: 1854-3928 print edition

www.Morana-rtd.com

e-PRESERVATIONScience

published by MORANA RTD d.o.o.

SCIENTIFIC PAPER

CHARACTERISATION OF LASER - INDUCED PHYSICAL ALTERATIONS OF PIGMENTED OIL LAYERS

Rui Bordalo[1]*, Paulo J. Morais[2], Christina R.T. Young[3], Luís F. Santos[4], Rui M. Almeida[4]

This paper is based on a presentation at the 2nd International Conference "Matter and Materials in / for Cultural Heritage" (MATCONS 2011) in Craiova, Romania, 24-28 August 2011.

Guest editor:
Prof. Dr. Elena Badea

1. Universidade Portucalense, R. Dr. António Bernardino Almeida, 541, 4200-072 Porto, Portugal
2. Instituto de Soldadura e Qualidade, Taguspark-Oeiras, Av. Prof. Dr. Cavaco Silva 33, 2740-120 Porto Salvo, Portugal
3. Conservation and Technology Department, Courtauld Institute of Art, Somerset House, Strand, London, WC2R ORN, United Kingdom
4. Departamento de Engenharia de Materiais / ICEMS, Instituto Superior Técnico / TU Lisbon, Av. Rovisco Pais, 1049-001 Lisboa, Portugal

corresponding author:
rmbordalo@gmail.com

received: 31.12.2011
accepted: 04.11.2012

key words:
laser cleaning, excimer, pigments, oil, SEM, AFM

There has been a growing interest since the mid-1990s in the use of lasers as an alternative method of cleaning of painted surfaces to surpass the possible problems of irreversible modification caused by chemical or mechanical methods. The objective of this research is to extend the current understanding of excimer laser-induced discoloration effects on pigments mixed in oil medium. The study focuses on the response of samples of pure pigments and their mixtures widely used by painters in the nineteenth century, to different laser parameters. Characterisation of physical changes was performed using optical microscopy, colorimetry, scanning electron microscopy, and atomic force microscopy. It has been found that materials have different sensitivity to irradiation at 248 nm and that even if an ultraviolet wavelength is used, the photo-chemical mechanism may not be the predominant effect. The effect of irradiation on a pigment mixture cannot be predicted from the effect of the irradiation on the individual pigments.

1 Introduction

Over the last decades, laser cleaning has been widely studied and has started to be used in the conservation of works of art.[1-4] Since the mid-1990s, there has been a growing interest in the use of lasers in the cleaning of painted surfaces and hence considerable research has taken place.[5-7] However, these studies have revealed that the paint can degrade or change its surface morphology by laser radiation, due to its multiple layers and heterogeneous nature. The greatest disadvantage of laser cleaning is that under laser radiation, painting materials can experience undesirable physical and chemical alterations such as pigment discoloration or medium degradation.[8-9] The constituent materials react to laser radiation in different ways, depending on their chemistry. Laser-matter interaction depends both on the properties of laser radiation and on the intrinsic properties of the material surface. Artwork cleaning by laser interaction can be explained by three major mechanisms: thermal, photomechanical and photo-chemical, which may occur at the same time although one is normally predominant depending mainly from the wavelength used.[10]

In varnish removal, it has been observed that the high energy pulse of the KrF excimer laser (248 nm) is adequate for material ablation since the energy results in a photochemical action that breaks the atomic bonds of

organic materials. In fact, research has shown that 248 nm is the most promising wavelength for varnish and overpaint layer removal.[11,12] UV radaition is strongly absorbed by the traditional varnish functional groups and its degradation products. In partial removal there is a minimal thickness that should remain intact to prevent any radiation to be absorbed by the underlying layers. However, further research into the discoloration of the paint layer in case of direct laser irradiation has yet to be carried out. Previous research has focused mainly on direct laser irradiation of real paintings or of pigment samples, either in the form of powder or mixed within a medium but not in a systematic way.[7,13-17] The present study compares the physical changes of pigment mixtures to those of pure pigments. This approach was chosen in order to better understand the behaviour of the paint samples which more closely represent real paintings. Previous studies of the laser effects on most of these pigments have been limited.

2 Experimental

2.1 Sample Preparation

A comprehensive list of inorganic pigments in use in the 19th century was compiled from different sources. Next, the pigments were categorised according to their colour and chemical nature. From among the pigments used during the nineteenth century, priority was given to those that were also used in previous centuries, which was desirable in order to obtain results as broad and useful as possible. Also, the pigments had to belong to different colour families (black, white, yellow, red and green), so that their mixtures would be unique and visually distinguishable. Finally, the pigments had to be as different as possible in their chemical nature in order to achieve a wide representativity of the chemical pigment families. A fourth condition, desirable but non-compulsory, was the lack of previous studies on the laser effects. Initially, a set of seven inorganic pigments were considered but an organic one was added to provide a potentially useful behaviour comparison between organic and inorganic pigments and because laser-induced effects in organic pigments are still an important gap in the current state-of-the-art. After considering a large list of pigments used in the 19th century, the following were chosen: lead white, yellow ochre, chrome yellow, vermilion, viridian green, Prussian blue, bone black and rose madder. The binding medium was cold-pressed linseed oil. The pigments were produced according to historic recipes and obtained from Kremer Pigmente (Germany) and AP Fitzpatrick (United Kingdom).

The samples were made according to the traditional technique of oil paint preparation by grinding pigment in oil on a stone plate. Linseed oil was added in the ratio of typically 3-4 ml of oil per 2 g of pigment, to obtain a mixture fluid enough to be easily spread on the support. The paint was deposited over a flexible substrate (polyester film sheets 3M PP2280) with a manual film applicator (Neurtek) producing a 200 µm thick wet layer. Pure and mixed samples were prepared: a total of eight pure pigments and 16 binary mixtures (in a 1:1 ratio).

The samples were then left to dry for two months in normal ambient conditions and then placed in a photo-degradation chamber equipped with UV-filtered fluorescent daylight tubes to simulate ageing in a museum. The samples were left in these conditions for 8 months during which the ageing is assumed to be equivalent to approximately 110 years.

2.2 Laser System

The samples were then irradiated with a KrF laser Lambda Physic COMPex 110. This laser operates at a wavelength of 248 nm, with 30 ns pulse duration at 2 Hz frequency. After emission, the laser beam was shaped by a mask of 11 x 5 mm and focused by a 150 mm focal length quartz plano-convex lens. For easy control of the samples, they were placed on a manual X-Y translation stage.

Before irradiation, preliminary tests were performed in order to determine the sensitivity and to make an early prediction of the behaviour of the samples. Based on the results, the samples were irradiated at varying fluence (F), from F = 0.001 J/cm^2 to F = 0.4 J/cm^2, at 1, 3 and 5 pulses, and occasionally 10 pulses to determine the discoloration and ablation thresholds.

2.3 Analytical Techniques

The samples were analysed before and after laser irradiation using several analytical techniques for their chemical and physical characterisation. In particular, the samples were analysed by optical microscopy, colorimetry, scanning electron microscopy, and atomic force microscopy. Due to the large amount of collected data per sample, only the most relevant results will be discussed.

Visual analysis was performed with a high resolution Carl Zeiss Axiotech 100HD-3D microscope. A Canon PowerShot G5 digital camera was coupled to the microscope. The photographs were taken with shutter speed 1/60 s, lens aperture F/4 and focal length 16 mm.

The colour was measured by a Konica-Minolta CM-2600d spectrophotometer under normal ambient conditions and with the following operating conditions: specular component included, UV excluded, illuminant D65 and 10° standard observer. The data was analysed with SpectraMagic NX software. The reported CIELab coordinates are the average of three measurements on each sample.

Scanning electron microscopy in combination with energy dispersive X-ray analysis (SEM-EDX) was performed on a Hitachi S-2400 scanning electron microscope with a standard EDX detector from Bruckër (ex-Rontec). The samples were gold-coated to improve surface conduction, and the images were taken at 25 kV with a spot size of ~1 nm and using software Multi Image 2.1.

The topographic characterization of some of the film samples was made using a Veeco DI CP-II Atomic Force and Scanning Tunneling Microscope. The system is equipped with a 50 x 50 µm scanner stage and

a motorized Z stage, and it was connected to a PC enabling computer control and data acquisition with software Proscan 2.1.

3 Results

One of the first objectives was the determination of the discoloration and ablation thresholds. The discoloration threshold was first identified by naked eye and then quantified using a spectrophotometer to determine its colour change (ΔE CIE 1976). The ablation threshold was determined by optical microscopy, analysing the surface at 50x and 500x. The samples revealed gradual laser-induced effects and thus a threshold range is determined. The threshold was found by irradiating the samples at consecutively higher fluences, each one also at increasing number of pulses (1, 3, 5, and 10) to determine a smallest range in combination with varying fluence. The exact ablation thresholds of each sample have been published elsewhere[17]. The set of eight pigments can be distributed in three ranges according to their ablation thresholds: a) $0.18 < F < 0.2$ J/cm^2, 1 to 5 pulses; b) $0.26 < F < 0.29$ J/cm^2, 1 to 5 pulses; and c) $F > 0.4$ J/cm^2. The lowest fluence range is where most of the pigments (five) have their ablation threshold. Parallel to the samples, a sample of oil without pigments was irradiated and it was verified that the ablation of oil is promoted by the presence of pigments.

3.1 Lead White (LW100)

Lead white is one of the pigments with the lowest discoloration threshold and very sensitive to becoming grey or black. Lead white is an unusual pigment with respect to its behaviour upon laser irradiation. It is known that the discoloration of lead white diminishes with time but literature does not report the degree of recovery. It was found that the colour recovery is dependent on the energy incident on the surface. Immediately after irradiation, the sample exhibited a colour change of up to ΔE = 30 although a permanent discoloration of ΔE = 13 was measured after two weeks. Although colour variation less than ΔE ≤ 1 is considered hardly visible by the human eye, most of the permanent discolorations of the sample were perceived.

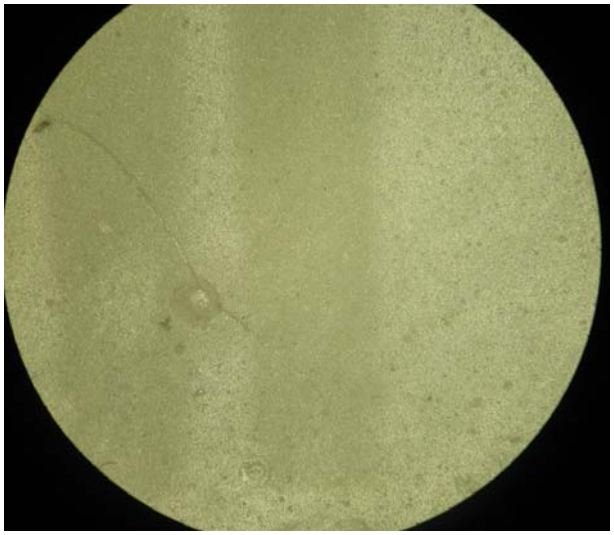

Figure 1: Micrograph of an area of LW100, permanently affected by laser irradiation at F = 0.1 J/cm^2 and 5 pulses, in reflected-light bright field (magnification 200x).

Figure 1 shows an area irradiated using different laser parameters (vertical shadows in the centre), after colour conversion, which was found to be permanent after two weeks. SEM analysis was performed but the comparison between the non-irradiated and the irradiated area at F = 0.36 J/cm^2 did not reveal any changes even at higher magnifications of up to 15,000x. The absence of distinctive differences between the non-irradiated and the irradiated areas suggests that the colour change induced by laser radiation in lead white is not accompanied by any physical change, leading to the conclusion that it is of a purely photo-chemical nature.

3.2 Yellow Ochre (YO100)

Yellow ochre is the only earth pigment among the set of pigments in the study. As expected, it revealed higher resistance to laser-induced alterations in comparison with the other pigments.

SEM imaging confirmed that laser irradiation at low fluence increased surface roughness, even though it may be invisible to the naked eye. Figure 2 shows the difference between the original surface and the irradiated area at F = 0.36 J/cm^2. The non-irradiated area is smooth and shows little topography (Figure 2A) while the irradiated area is quite uneven (Figure 2B). The precise photo-mechanic mechanism of this alteration is unknown although it could be due to melting or due to a surface rearrangement mechanism.

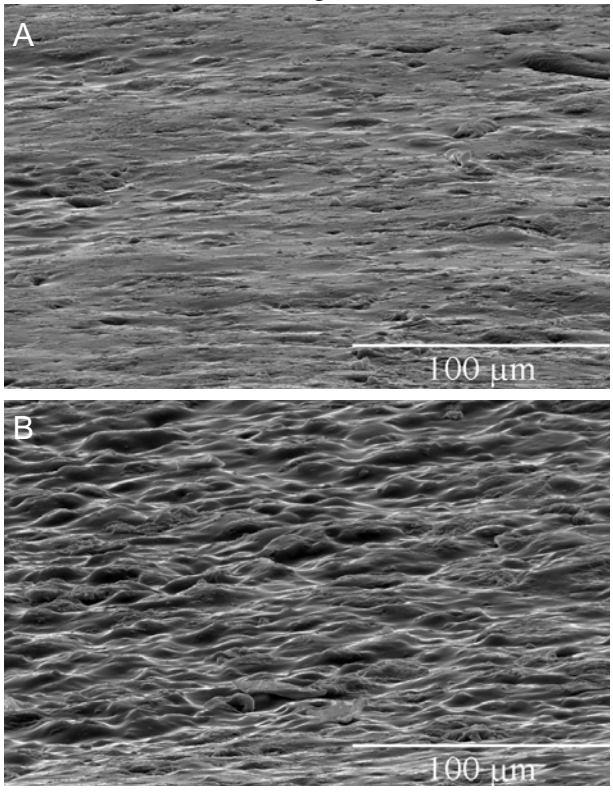

Figure 2: Scanning electron micrograph of the characteristic surface of a non-irradiated area (A) and of an irradiated area at F=0.36 J/cm^2 (B) of yellow ochre (YO100). Reproduced with permission from ref. 17.

3.3 Chrome Yellow (CY100)

When observed through the optical microscope, the irradiation tests were only perceptible in bright field mode. After laser irradiation, only the SEM image at 15,000x revealed a perceptible alteration. A comparative analysis of the highlights of individual areas can be seen in Figure 3. In the non-irradiated area the pigment particles were well embedded in the oil matrix, while in the irradiated area the particles were at the surface because of the removal of a superficial oil layer.

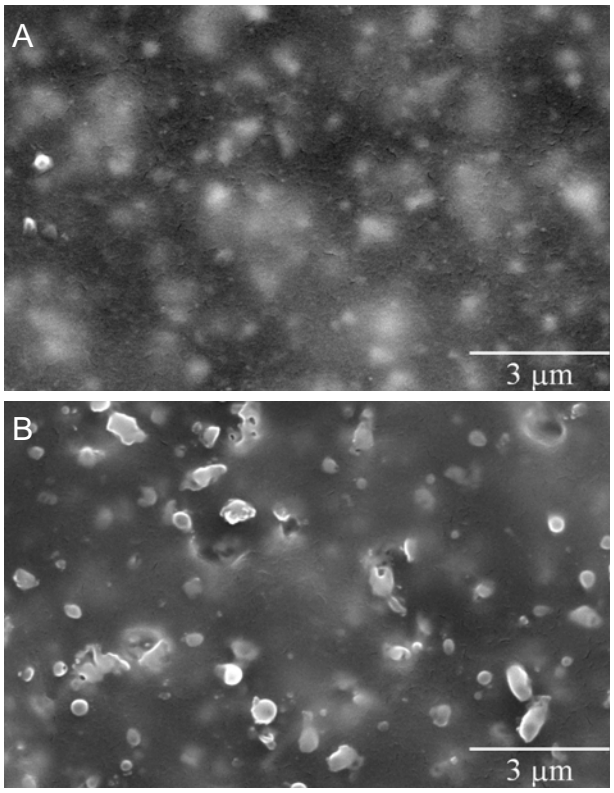

Figure 3: Scanning electron micrographs at 15,000 x of chrome yellow (CY100): non-irradiated area (A), and irradiated area (B). Reproduced with permission from ref. 17.

3.4 Viridian Green (VG100)

Viridian green has one of the highest discoloration thresholds of all pigments as shown by the relatively low colour change of ΔE = 1.7 at a fluence of F = 0.15 J/cm^2 and 3 pulses.

Comparative analysis between areas before and after laser irradiation seems to indicate that no ablative process took place since both surfaces are similarly smooth (Figure 4). However, the irradiated area shows a layer of particles with an approximate size of 1-5 µm deposited over the surface. These were deposited onto the surface after laser irradiation although their origin is not clear since there are no surface craters or other modifications that can explain the source of the particles. Figure 5 shows the general topography of the irradiated (left) and non-irradiated (right) areas. The presence of the particles is almost imperceptible here, in comparison with the sample topography.

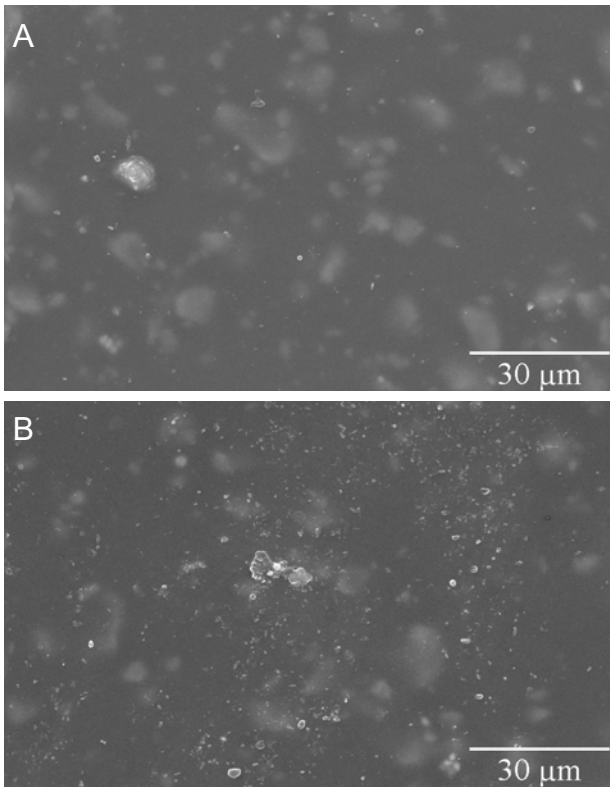

Figure 4: Scanning electron micrograph of viridian green (VG100): non-irradiated area (A), and irradiated area (B) at F = 0.36 J/cm^2.

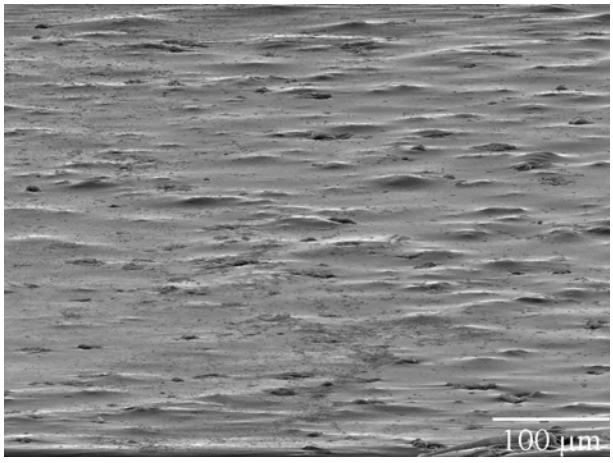

Figure 5: Scanning electron micrograph at 80º of the irradiated and non-irradiated areas of viridian green (VG100). Reproduced with permission from ref. 17.

3.5 Vermilion (V100)

Upon laser irradiation, vermilion typically turns to grey and black. The pure pigment sample (V100) showed a discoloration threshold of F=0.03 J/cm^2, which was the lowest in comparison with all the other pigments but presented the highest colour variation, with ΔE = 17.8 at F = 0.36 J/cm^2.

Two different areas of V100, a non-irradiated and an irradiated one, were analysed by AFM. Figure 6 shows 3D micrographs of the surface of V100 before and after laser irradiation at F = 0.36 J/cm^2. The estimated root mean square roughness (Rrms) was 400 nm and 349.5 nm for the non-irradiated and the irradiated areas, respectively. However, this difference is

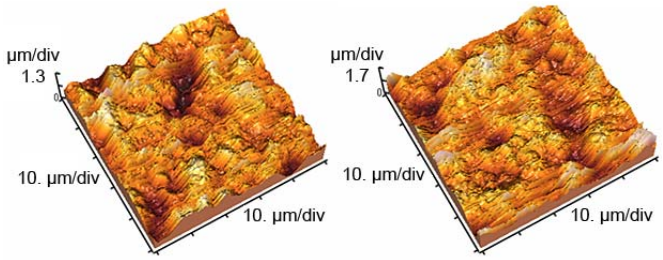

Figure 6: AFM 3D micrographs (50 x 50 µm) of V100 before (left) and after laser irradiation (right).

not conclusive as it may be due to the different locations where the analyses were performed.

3.6 Rose Madder (RM100)

Rose madder is the only organic pigment from the set and it was expected to show good resistance to laser irradiation due to its organic composition. The colour change of the pigment is one the lowest among the pigments studied, with a colour variation that ranges from ΔE = 2.1 to ΔE = 2.6. The irradiated area is very similar to the non-irradiated one except for a higher concentration of particles deposited on its surface (Figure 7).

Rose madder has a high discoloration threshold, undergoing discoloration at a fluence of approximately 0.28 J/cm^2. The laser-induced alteration was difficult to assess. Optical microscopy and SEM images suggested only slight discoloration.

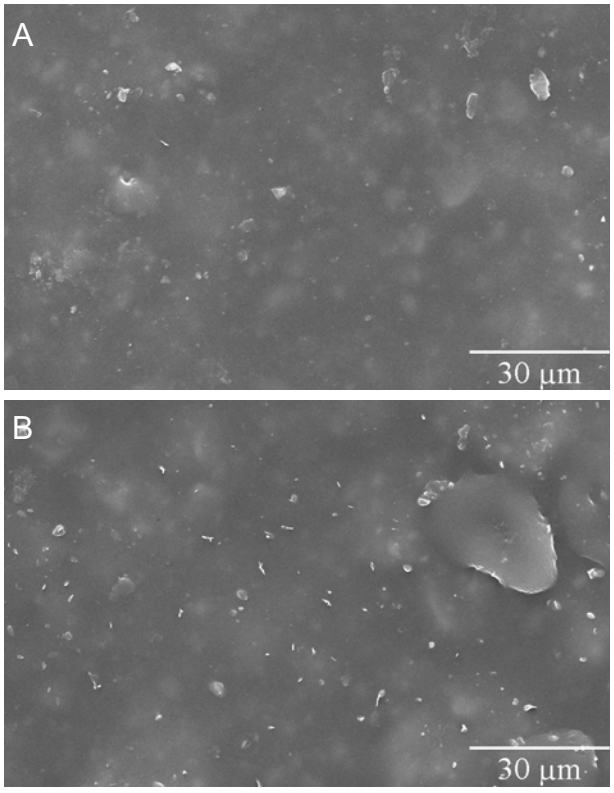

Figure 7: Scanning electron micrographs of rose madder (RM100). Visual comparative analysis shows that there is no alteration in the surface between the non-irradiated surface (A) and the laser irradiated surface at F = 0.36 J/cm^2 (B).

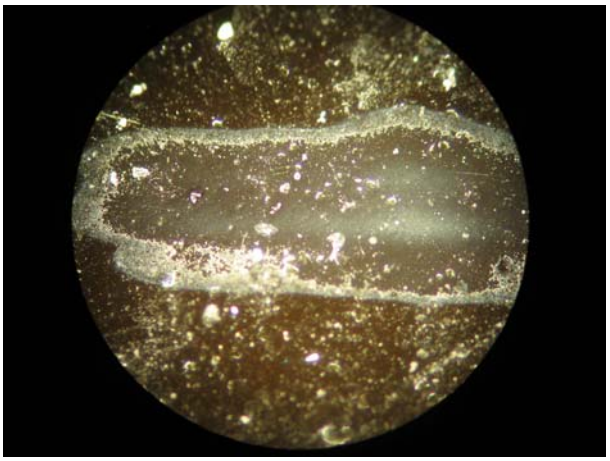

Figure 8: Micrograph of the effect induced by laser irradiation of PB100 at F = 0.2 J/cm^2 and 3 pulses (magnification 100x) in dark field contrast.

3.7 Prussian Blue (PB100)

Prussian blue is among the most sensitive pigments to discoloration and has an average resistance to ablation when compared with the other pigments in study. The colour variation of Prussian blue is unique as it changes very easily to different tones of blue and dark grey according to the differences in the beam energy density (Figure 8). It was also the only pigment where plasma was observed during laser irradiation. Prussian blue exhibited most intensive discoloration, ranging from ΔE = 1.9 to ΔE = 8.4, but had an average response to ablation when compared with the other pigments.

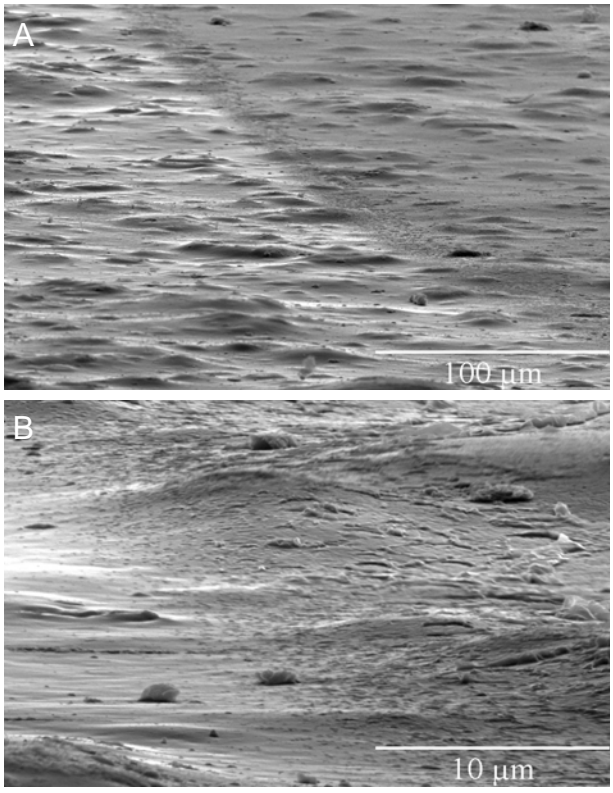

Figure 9: Scanning electron micrographs of Prussian blue (PB100) at 80º. Figure A shows the border area between the non irradiated area (lower left) and the irradiated area (top right) at F = 0.36 J/cm^2. Figure B shows in detail the physical laser-induced alterations at the border area alone.

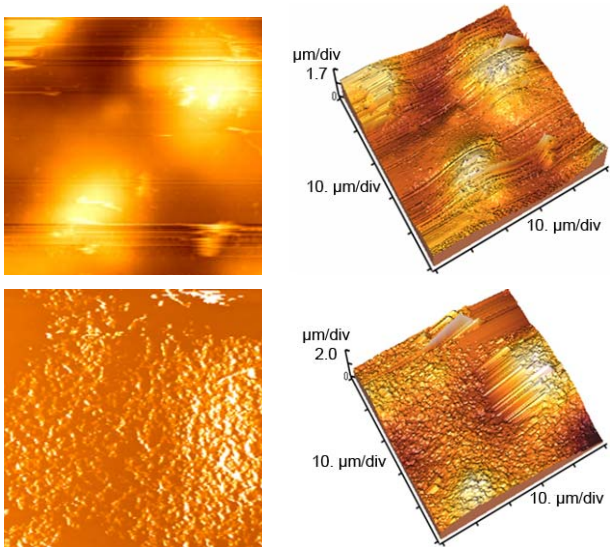

Figure 10: AFM 2D and 3D micrographs (50 x 50 µm) of PB100 before (above) and after laser irradiation (below).

SEM imaging of the control sample revealed a smooth surface where the pigment particles are embedded into the medium and with some particles at the surface. However, significant alteration of the surface is observed. Unlike other samples, visual comparison between two different areas shows a significant difference. Figure 9A shows a small area of PB100 irradiated at F = 0.36 J/cm^2 oriented at 80º and focused at the interface of the irradiated area. Laser ablation is obvious in this area, as can be observed in the detail in Figure 9B. However, a similar effect was not observed for the irradiated area, despite the fact that the surface seems smoother and more regular than that of the non-irradiated area.

AFM analysis was performed on PB100 in order to assess the topographic alterations that laser irradiation induced to the sample surface. For the analysis, two areas were selected from nearby the borderline between both zones. Figure 10 shows 2D and 3D micrographs from the surface of PB100 before and after laser irradiation at F = 0.36 J/cm^2. The topographical difference after laser irradiation is obvious in both 2D and 3D micrographies. The surface roughness (Rrms) for the non-irradiated surface (492 nm) decreased after laser irradiation (357 nm).

3.8 Bone Black (BB100)

Bone black revealed to be the least sensitive pigment to laser irradiation with higher discoloration and ablation thresholds than any other pigment in the present study. At a relatively high fluence such as F = 0.2 J/cm^2 the colour variation was still under ΔE < 1. The discoloration is towards a dark grey and the colour variation is small, ranging from ΔE = 0.2 to ΔE = 3.2. SEM imaging show no changes on the sample surface even at a high fluence such as F = 0.36 J/cm^2.

3.9 Lead White-Yellow Ochre (LW50-YO50)

SEM imaging confirmed that the oil medium has been removed leaving a surface of unprotected pigment particles. Figure 11 shows the difference between the original surface (Figure 11A) and the irradiated area at F = 0.36 J/cm^2 (Figure 11B) of LW50-YO50. The most obvious difference between the micrographs is the removal of the most superficial layer of the medium, apparently leaving the pigment particles without the binder. This difference, however, is not well appreciated at lower magnifications.

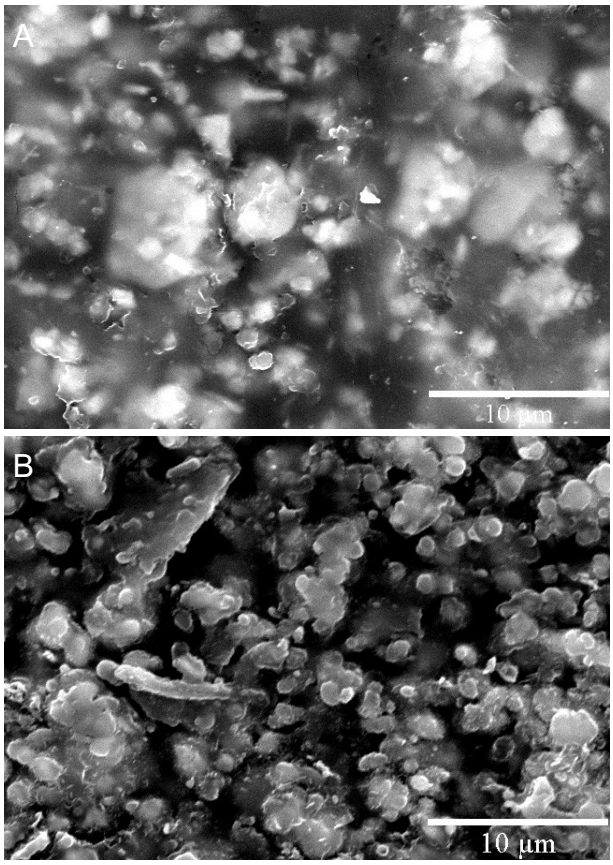

Figure 11. Scanning electron micrograph of the characteristic surface of a non-irradiated area (A) and of an irradiated area at F=0.36 J/cm^2 (B) of LW50-YO50.

3.10 Lead White-Chrome Yellow (LW50-CY50)

Direct comparison using SEM imaging of the non-irradiated and the irradiated areas at 80º (Figure 12) suggests that this alteration is due to the lifting of small flakes instead of the oil layer removal. Figure 12B shows several particles of different sizes and shapes scattered over the irradiated surface. It is not possible to assess if the particles remained on the surface after selective removal of the binder or if they were deposited on the surface during or after the irradiation process.

The comparison between this mixture and the pure pigments in its composition does not reveal any special similarity. SEM imaging of LW100 did not reveal any laser-induced effect although CY100 revealed a comparable situation with that shown in Figure 12. However, the pigment particles that are observable in the present case are much bigger than in case of CY100. Thus, there seems to be no particular laser-induced effect on the pigment.

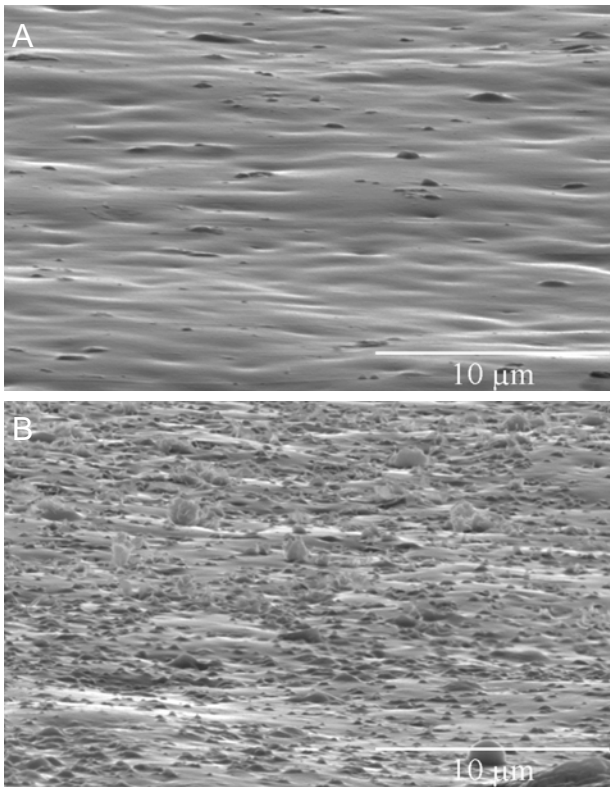

Figure 12: Scanning electron micrograph at 80º of the characteristic surface of a non-irradiated area (A) and an irradiated area at F=0.36 J/cm^2 (B) of LW50-CY50.

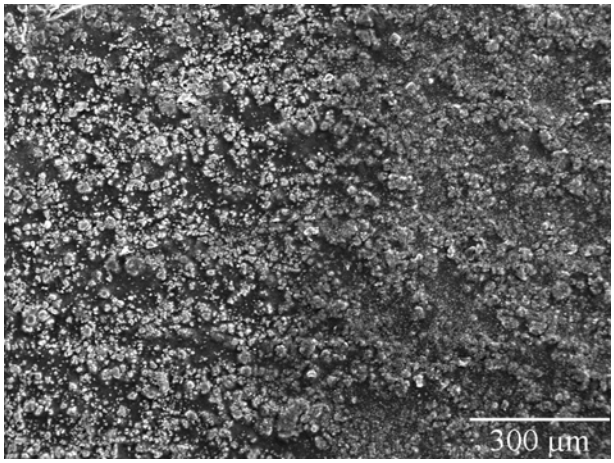

Figure 13: Scanning electron micrograph of LW50-VG50. The image highlights the borderline between the non-irradiated and the laser irradiated surface at F = 0.36 J/cm^2.

3.11 Lead White-Viridian Green (LW50-VG50)

The mixture of lead white with viridian green did not undergo chemical degradation and colorimetry showed that the mixture is less sensitive than its pure pigments. The reason why a certain mixture has a higher discoloration threshold than its component pigments could not be explained but it is clearly pigment dependent. Colorimetry analysis concluded that the mixture has its discoloration threshold in the range between the respective thresholds of its pure pigments.

Figure 13 shows a SEM micrograph where the irradiated (A) and non-irradiated (B) borderline is highlighted. Further analysis at a higher magnification showed that the reason for the perceptible difference is the removal of the binder at the surface. Nevertheless, there is no evidence that the pigment was affected. The mixture presents a different behaviour than that of the pure pigments alone. While lead white did not show any physical alteration, viridian green revealed only some particles that were apparently deposited on the surface, leaving the surface top layer undamaged.

3.12 Lead White-Vermilion (LW50-V50)

Although the mixture contains lead white and vermilion, which are the most sensitive pigments in the ensemble, the mixture was relatively unaffected by laser irradiation. Indeed, the mixture (discoloration threshold at F = 0.1 J/cm^2) is less sensitive than the pure pigments as lead white and vermilion have discoloration thresholds at F = 0.05 J/cm^2 and at F = 0.03 J/cm^2, respectively. This is confirmed by colorimetry, which upon irradiation at F = 0.085 J/cm^2 showed a negligible discoloration of ΔE = 0.4.

The comparison of the surface between the non-irradiated and the irradiated area at F = 0.36 J/cm^2 can be observed in Figure 14. The topographic aspect of the surface prior to laser irradiation (Figure 14A) is very smooth with only a few regularly distributed orifices that may be related probably to the release of air bubbles while drying. On the other hand, the irradiated area (Figure 14B) reveals that ablation took place leaving a highly rough and irregular surface.

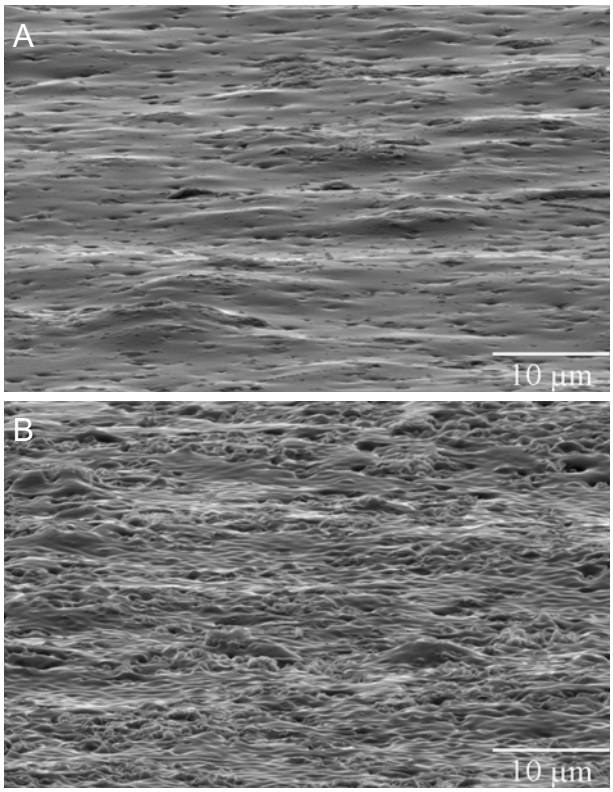

Figure 14: Scanning electron micrographs of LW50-V50. Figure A shows the topographic aspect of the surface prior to laser irradiation while Figure B shows the physical changes that the sample undergo after laser irradiation at F = 0.36 J/cm^2.

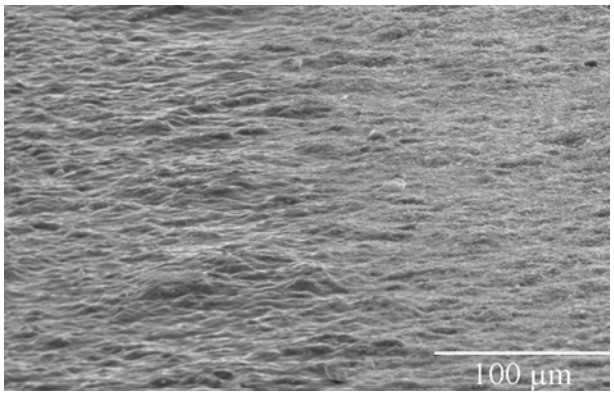

Figure 15: Scanning electron micrograph of LW50-RM50. It is possible to observe the interface area between the non-irradiated area (left) and the irradiated (right) area at F=0.36 J/cm^2 (B).

Figure 16. Scanning electron micrograph of LW50-RM50, detail of the interface from Figure 15.

3.13 Lead White-Rose Madder (LW50-RM50)

In the case of rose madder, the mixture with lead white increased the sensitivity of the organic pigment. Laser radiation had a singular effect on LW50-RM50 at microscopic level, observable by SEM imaging. Figure 15 shows the borderline between the non-irradiated (left) and the irradiated (right) areas. The natural roughness of the surface can be observed in the left part whereas the irradiated part is presented as a flatter surface. A detail of the borderline can be seen in Figure 16 where it is clear that the laser radiation induced localized bursts resulting in the alteration of the surface although the exact alteration mechanism is unknown. This effect, unlike the reactions of either rose madder or lead white alone, is probably a photo-mechanical mechanism. A similar reaction was also observed in other mixtures such as LW50-BB50.

3.14 Lead White-Prussian Blue (LW50-PB50)

The laser-induced change to Prussian blue is very characteristic. However, unlike the behaviour of the pure pigment, its mixture with lead white produces a different discoloration towards a darker tone, undoubtedly due to the presence of lead white. The discoloration threshold of this mixture is within the range between the pure pigment thresholds.

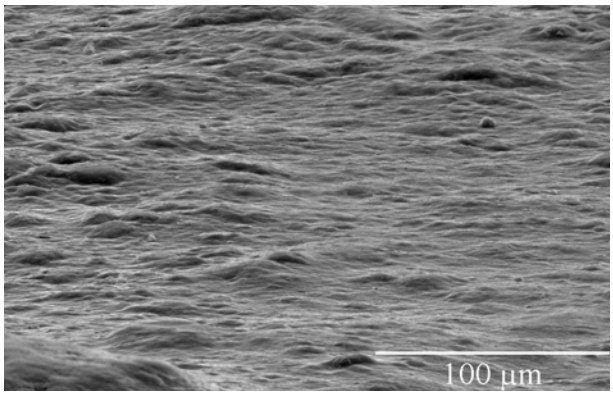

Figure 17: Comparative scanning electron micrograph of the characteristic surface of an irradiated area at F = 0.36 J/cm^2 (upper left) and of a non-irradiated area (lower right) of LW50-PB50.

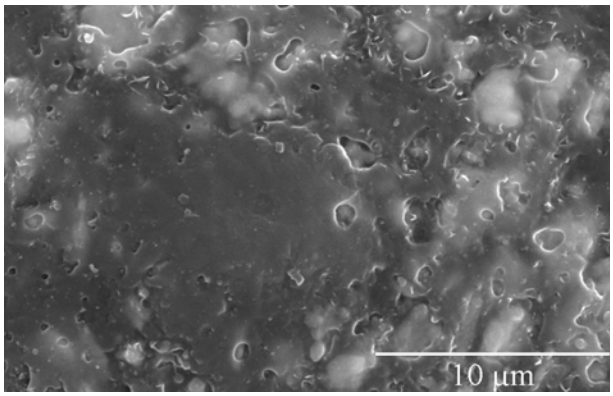

Figure 18: Macro view of the irradiated area of LW50-PB50 at F = 0.36 J/cm^2 showing numerous craters, not visible in the non-irradiated area, corresponding to the selective removal of the oil.

SEM imaging of the laser-induced alteration between the non-irradiated and the irradiated areas at F = 0.36 J/cm^2 (Figure 17) is evident even if the borderline is not very clear. It is evident that ablation took place in the upper left corner of the micrograph, leaving the surface uneven and rough. The irradiated area was observed at higher magnification revealing numerous craters which are not visible in the non-irradiated area corresponding to the selective removal of the oil (Figure 18). The creation of this crater was induced by laser irradiation, which seems to preferentially damage the surface of the binder rather than the pigment particles. It should also be noted that the effect on the medium seems to have a direct connection to the presence of pigment. In the micrograph (Figure 18) it can be observed that the areas with more craters are also those with a higher concentration of pigment particles while the smoother areas correspond to a higher concentration of the binder. The neighbouring areas appeared similar. A suitable explanation for this mechanism could not be found.

3.15 Lead White-Bone Black (LW50-BB50)

As expected, the discoloration threshold of this mixture is between those of the pure pigments. However, the mixture exhibits higher discoloration for lower fluences than the ones of bone black. This means that its behaviour is closer to that of lead white than to that of bone black.

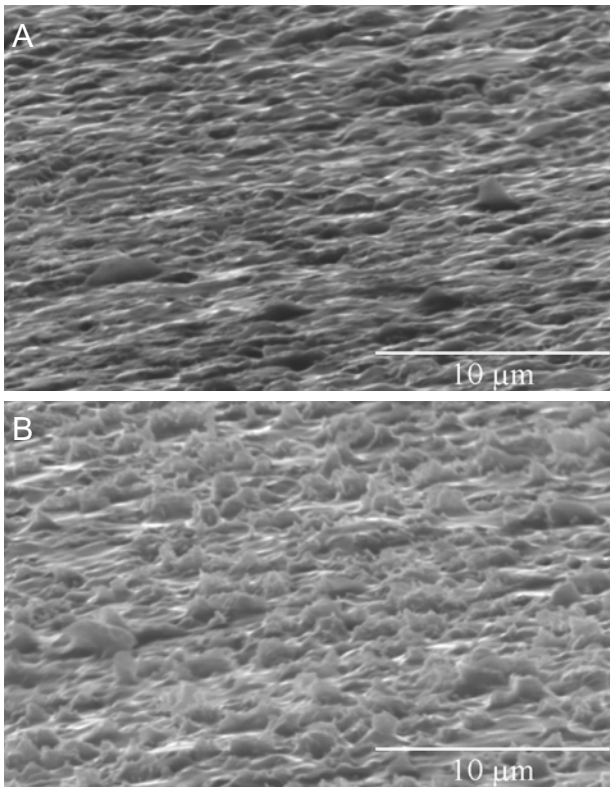

Figure 19: Scanning electron micrograph at 80º of the characteristic surface of a non-irradiated area (A) and of an irradiated area at F = 0.36 J/cm^2 (B) of LW50-BB50.

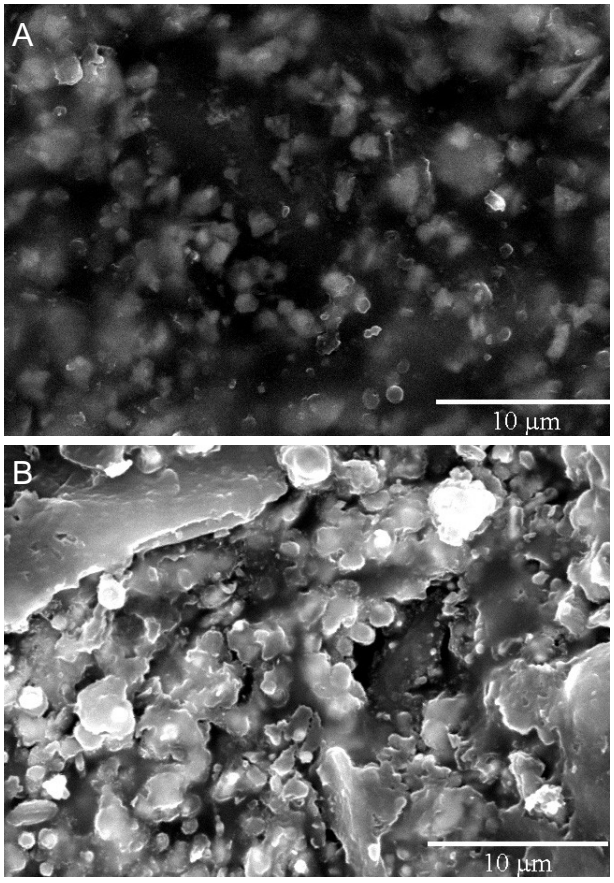

Figure 20: Scanning electron micrograph of YO50-PB50 aspect of the surface before (A) and after (B) laser irradiation at F = 0.36 J/cm^2.

Figure 19 compares the non-irradiated and the irradiated areas of the mixture at F = 0.36 J/cm^2. The irradiated surface appears to be very rough and irregular as the laser beam would have lifted some of the material in a burst.

3.16 Yellow Ochre-Prussian Blue (YO50-PB50)

The mixture shows a discoloration threshold that corresponds to the pigment with the lower threshold (Prussian blue, F = 0.08 J/cm^2) rather than an intermediate one between the discoloration thresholds for the pure pigments. Despite the lower discoloration threshold, the mixture shows an increasing resistance to higher fluences in comparison to the pure pigments alone.

SEM imaging showed that the laser radiation induced the removal of the top oil layer. The non-irradiated surface of the sample can be observed in Figure 20A where the pigment is regularly mixed in the binder and the surface is evenly smooth. After laser irradiation at F = 0.36 J/cm^2 (Figure 20B), it appears that the medium was partially and non-selectively removed from the surface, revealing the pigment particles underneath and leaving behind several flake-like areas of medium, giving a rough and uneven aspect to the surface.

3.17 Yellow Ochre-Bone Black (YO50-BB50)

As standard procedure, a view at low magnification and 80º was attempted but it was insufficient to obtain a perceptible view of the laser-induced effects. The surface of the non-irradiated and the irradiated areas are compared in Figure 21. The non-irradiated area appears as a flat and smooth surface where the pigment is embedded in the binder below the surface, except for some particles dispersed by the surface (Figure 21A). After irradiation the surface is uneven and characterized by a series of craters of different sizes created by the removal of the binder, leaving the pigment underneath uncovered (Figure 21B). Once again, the response of this mixture to laser irradiation has no similarity to the individual effects on the pure pigments in its composition.

3.18 Chrome Yellow-Vermilion (CY50-V50)

The mixture shows better resistance to laser radiation than its pure pigments. Although the difference between the non-irradiated and the irradiated areas is not strong, it is noticeable by the localized craters that characterize the irradiated area. The difference may be seen in more detail in Figure 22. In fact, the irradiated area is very similar to the non-irradiated one except for the localized craters that partially removed the binder leaving the pigment particles beneath uncovered. The craters are clean and no material is deposited around them or at the sample surface. The reason why they are so scattered is not known but it is suggested that the laser impact could lead to stress on the surface causing material to be

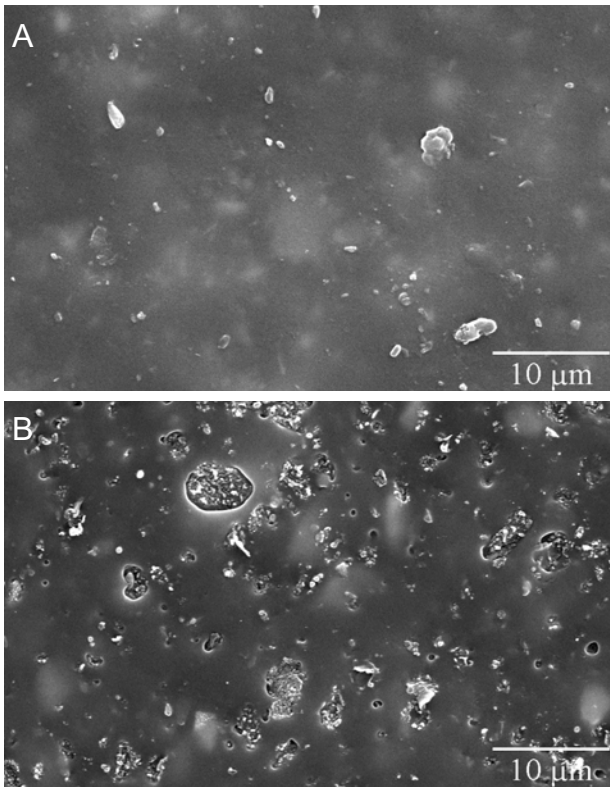

Figure 21: Scanning electron micrographs of YO50-BB50. Figure A shows the topographic aspect of the surface prior to laser irradiation while Figure B shows the physical changes of the surface after laser irradiation at F = 0.36 J/cm^2.

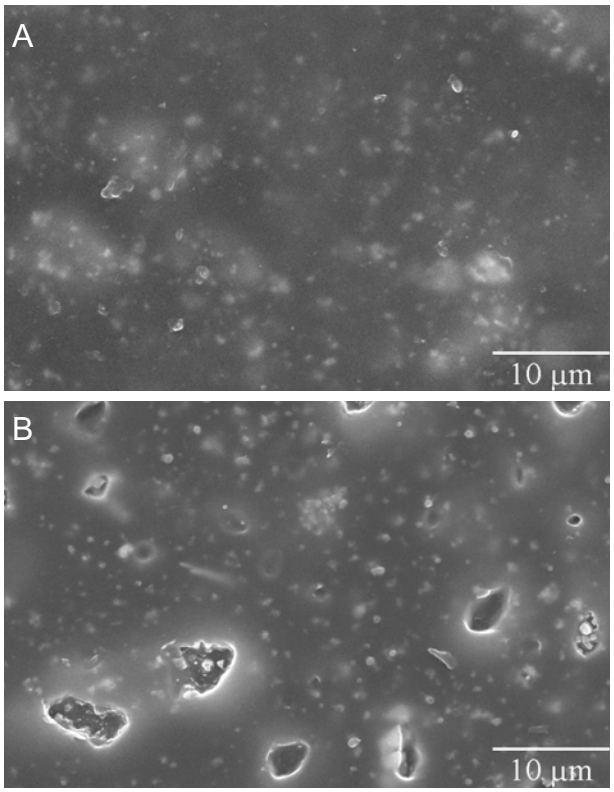

Figure 22. Scanning electron micrographs of CY50-V50. Figure A shows the topographic aspect of the surface prior to laser irradiation while Figure B shows the physical changes that the sample underwent after laser irradiation at F = 0.36 J/cm^2.

ejected in points of structural weakness. It should also be underlined, as shown in Figure 22B and by other details (images not shown), that all craters are surrounded by a halo.

3.19 Vermilion-Rose Madder (V50-RM50)

This mixture contains pigments with divergent sensitivity to laser radiation: rose madder has a high discoloration threshold while vermilion has the lowest discoloration threshold among the pigments in this study. Experimentally, it has been observed that the corresponding mixture has a slightly increased resistance to laser radiation.

Comparison of the SEM images of the irradiated and non-irradiated areas showed the main difference to be the presence of isolated craters on the top surface of the binder, similar to those observed in sample CY50-V50. The surface presents isolated punctures in the top layer of the binder while the pigment seems unaffected.

3.20 Vermilion-Prussian Blue (V50-PB50)

The discoloration of the mixture resembles that of pure Prussian blue. The mixture exhibits the same discoloration threshold as the most sensitive pigment in the mixture, vermilion, i.e. F = 0.05 J/cm^2. Nevertheless, the mixture shows higher resistance to laser radiation than vermilion at other fluences.

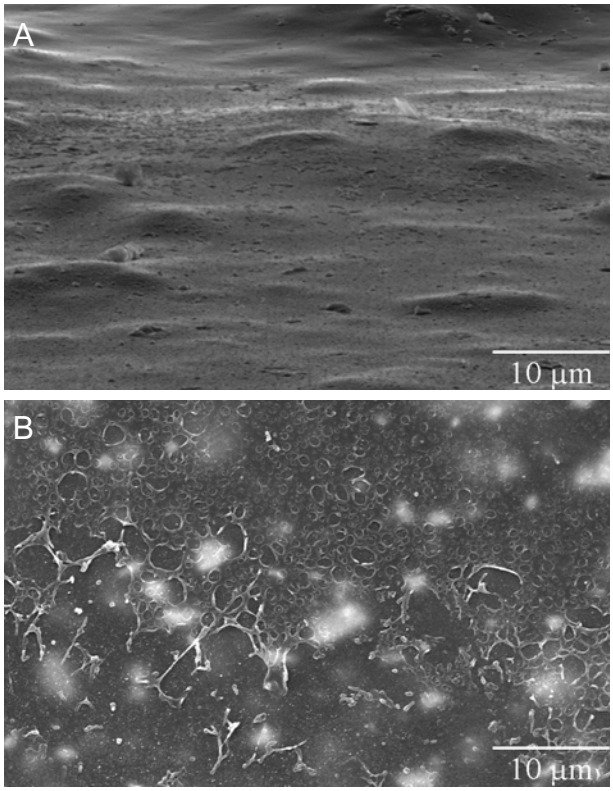

Figure 23: Scanning electron micrographs of V50-PB50 of the interface between the irradiated and the non-irradiated areas after laser irradiation at F = 0.36 J/cm^2. Figure A shows the topographic aspect of the surface at 80º while Figure B shows the same area from a perpendicular perspective.

SEM imaging showed that the laser-induced effect is limited to the superficial layers of the surface. The features shown in Figure 23 suggest that a superficial layer of the binder is altered or removed, leaving behind an almost identical surface with the exception of a few craters of minimum depth. This effect seems limited to the binder layer and the disrupted aspect allows the possibility of thermally induced degradation. The pigment seems to be unaffected by laser radiation.

3.21 Vermilion-Bone Black (V50-BB50)

The mixture is made of pigments with the lowest and highest discoloration thresholds among the pigments in the study. The laser-induced discoloration of this mixture is towards a 'burnt' darker tone. The comparison of the thresholds indicates a small influence of vermilion. Despite the fact that the mixture has a lower discoloration threshold than that of bone black, the results suggest that the mixture withstands better laser radiation at higher fluences.

Figure 24 compares two SEM micrographs from a non-irradiated and an irradiated area. The first (Figure 24A) is comparable with many other samples already analysed, where it is possible to see the pigment particles embedded in the binder and underneath the surface. On the other hand, the irradiated area shows a very disrupted surface (Figure 24B): the binder seems to have been removed leaving the particles underneath uncovered. The top of the pigment particles appears to have been affected as well. Upon laser irradiation at F = 0.36 J/cm^2, the top layer of the binder was removed leaving uncovered the pigment particles that underwent a severe disruption..

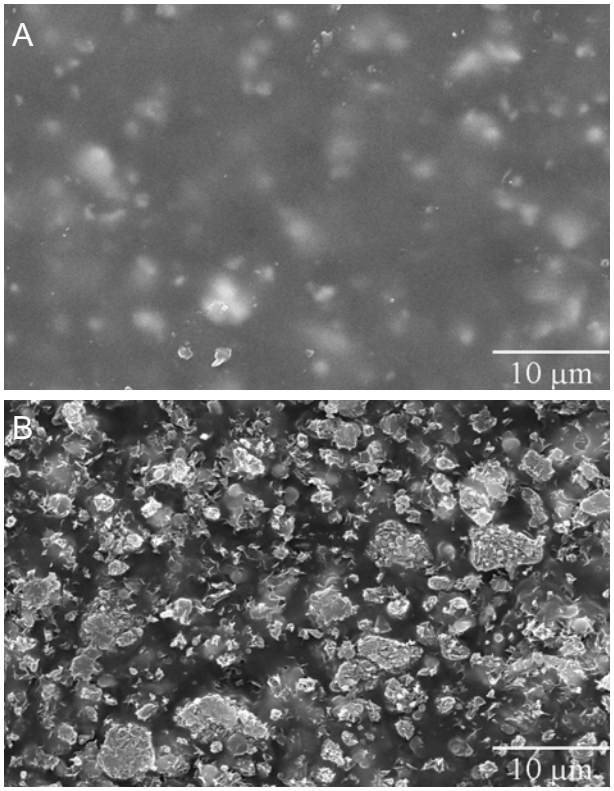

Figure 24: Scanning electron micrographs of V50-BB50. Figure A shows the topographic aspect of the surface prior to laser irradiation while Figure B shows the physical changes of the surface after laser irradiation at F = 0.36 J/cm^2.

3.22 Bone Black-Rose Madder (BB50-RM50)

This mixture includes pigments with the highest discoloration thresholds. Nevertheless, the mixture of both pigments presents a discoloration threshold below the threshold of any of the pure pigments. The laser-induced alteration of the sample surface can be appreciated in the borderline between the non-irradiated (lower right side) and the irradiated (upper left side) area at F = 0.36 J/cm^2 in Figure 25. The non-

Figure 25. Scanning electron micrograph of BB50-RM50 at 80º of the interface between the irradiated (lower) and the non-irradiated (upper) areas.

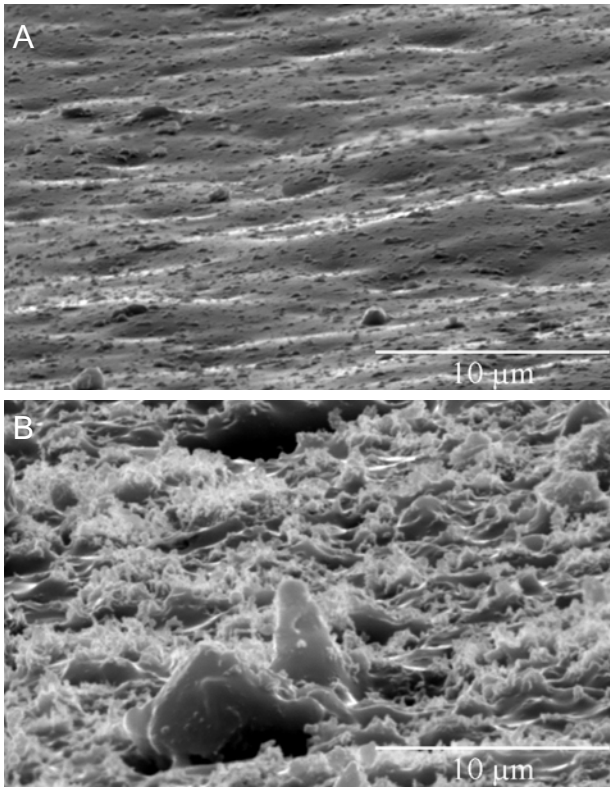

Figure 26. Scanning electron micrograph of BB50-RM50 at 80º of the characteristic surface of a non-irradiated area (A) and of an irradiated area at F = 0.36 J/cm^2 (B).

irradiated area appears smooth and flat as opposed to the irradiated one.

The irradiated surface (Figure not shown) shows severe damage: although the binder layer is still visible, the surface is disrupted by several particles, most probably pigment and binder elements. This is even more obvious at a higher magnification in Figure 26, where a detailed comparison of the laser-induced alteration is shown at a closer look at 80º. In particular, Figure 26B illustrates how the laser beam induced a burst of the top layer without ejection of the fractured material.

4 Discussion

According to Bordalo,[18] a sample can physicaly exhibit one of three possible stages upon laser irradiation: no perceptible modification, colour or morphological change on the surface, and ablation of the material. In a linear model, two thresholds would divide the three stages where one stage could evolve to the next one by increasing the laser fluence. However, this model is not accurate as it depends on material properties. In fact, one stage does not necessarily precede another. Therefore, there are two main thresholds, normally referred to in the literature, that should be considered and assessed: the discoloration and ablation thresholds. These thresholds are defined as the minimum amount of laser energy incident on the sample necessary to induce colour alteration or material removal from its surface, respectively. However, there is also another threshold that should also be considered for this specific application, which is the minimum amount of laser energy incident on the sample necessary to induce any physical alteration of the material surface.

One of the initial surprising effects was that many of the laser induced effects on the surface were visible by the naked eye but were not immediately obvious by optical microscopy. This is because of the scattering properties of the pigment and the angle of incidence of the light. It was necessary to observe many of the irradiated areas in bright field, dark field and polarized contrast in order to obtain the most accurate information.

Analysing the discoloration and ablation thresholds, it was also observed that the reaction of the mixtures does not follow a linear relationship with the reaction of their pure pigments. It has been observed that among the mixtures three types of reactions may take place; 1) the first and the expected reaction is when a mixture has the same or nearly the same ablation threshold as the pure pigments in its composition; 2) when the mixture shows a lower ablation threshold than that of its pure pigments; 3) when the mixture shows a higher ablation threshold than that of its pigments. The discoloration thresholds for all pigments are at relatively low fluences, between F = 0.03 J/cm^2 and F = 0.18 J/cm^2, except for bone black (BB100). The most sensitive pigments are lead white and vermilion which revealed similar behaviour: both undergo discoloration at a low fluence near F = 0.05 J/cm^2 and ablation near F = 0.20 J/cm^2. Chrome yellow was found to be the pigment with the smallest difference in the fluence between thresholds of only 0.05 J/cm^2. Among all the pigments, bone black proved to be the most resilient pigment to λ = 248 nm laser irradiation. Its discoloration threshold is slightly above the ablation threshold of the other pigments. Bone black (BB100) was irradiated at the maximum fluence possible with the laser set-up used (F = 0.40 J/cm^2) and still no ablation was observed.

The results also suggest that in some cases the addition of pigments, such as viridian green, to other pigments decreases the sensitivity of the mixture to laser-induced degradation. This was evident, for example, in the mixture of yellow ochre with viridian green which showed less discoloration even when irradiated at higher fluences. However, this fact would have to be studied further in a more comprehensive study involving several pigments.

5 Conclusion

This research presents a study of the physical effects of KrF excimer laser (248 nm) on a selected group of organic and inorganic pigments extensively used in the 19th century. The study aimed at a more comprehensive understanding of the physical and chemical effects, by analysing the pigments and their mixtures before and after irradiation. Optical microscopy, scanning electron microscopy, and atomic force microscopy were used to analyse the samples before and after the irradiation. The experimental results are expected to serve as a basis to further research and laser applications on laser cleaning of paintings as well as to help to establish working procedures and safety limits in future applications.

SEM analysis was a valuable characterisation technique because it allowed detailed observation of the laser-induced effects on the sample surface, even when the effects were not visible by naked eye. From SEM analysis one can conclude that laser irradiation had different effects at very different levels on the surface, depending on the sample. These differences ranged from minimum changes to a complete modification of the topography and roughness of the surface. The most common effect was removal of the top layer of the binder, leaving behind a surface of unprotected pigment particles. Interestingly, there were several samples that revealed quite unexpected effects such as, e.g., the mixture LW50-PB50 which showed laser-induced craters on its surface.

The mixtures show a behaviour which is very different from the pure pigments, suggesting that each pigment has a different influence on the behaviour of the mixture. Several material or physical factors may influence the physical effect that laser radiation has on the surface of the samples. Particle size is one of those factors. For example, the difference between YO100 and CY100 is consistent with the different particle sizes for both pigments.

The predominant degradation mechanism of organic materials by ultraviolet radiation is photo-chemical, inducing scission of covalent bonds. It is suggested that most of the differences observed by SEM are due to different degradation mechanisms. It has been reported that the photo-chemical mechanism is the predominant one with UV lasers. However, SEM analysis suggests that the photo-mechanical and photo-thermal mechanisms are also present. While most

samples do not show any sign of predominant thermal processes, some samples showed a type of disruption of the surface which is associated with mechanical stress during laser irradiation. This photo-mechanical degradation was much greater than expected.

The results for the mixtures of pure pigments showed that their behaviour may not be assumed to be an average of their pure pigments. In fact, either physically or chromatically, the mixtures showed different and sometimes unexpected behaviour.

6 Acknowledgments

Fundação para a Ciência e Tecnologia (BD/16759) is gratefully acknowledged for funding the PhD research (Courtauld Institute of Art, London). The participants in the national project LASARTE ("Tecnologia Laser em Materiais Pictóricos", project nº 70/00343), funded by ADI, are also acknowledged.

7 References

1. J. F. Asmus, G. Guattari, L. Lazzarini, G. Musumeci, R. F. Wuerker, *Holography in the Conservation of Statuary*, Stud. Conserv. 1973, **18**, 49-63.

2. J. F. Asmus, C. Murphy, W. Munk, *Studies on the Interaction of Laser Radiation with Art Artifacts*, Proc. Soc. Photo-opt. Instr. Eng. 1973, **41**, 19-27.

3. L. Lazzarini, J. F. Asmus, *The application of laser radiation to the cleaning of statuary*, Bull. Am. Inst. Conserv. Hist. Art. Works 1973, **13**, 39-49.

4. J. F. Asmus, *More light for Art Conservation*, IEEE Circuits and Devices Magazine, 1986, **2**, 6-14.

5. C. Fotakis, E. Hontzopoulos, I. Zergioti, V. Zafiropulos, M. Doulgeridis, T. Friberg, *Laser Applications in Painting Conservation*, in: 1995 Paintings Specialty in 1995 AIC Paintings Specialty Group Postprints, J.H. Gorman (ed.), The American Institute for Conservation of Historic and Artistic Works, Saint Paul, 1996, pp. 36-42.

6. I. Zergioti, A. Petrakis, V. Zafiropulos, C. Fotakis, A. Fostiridou, M. Doulgeridis, *Laser Applications in Painting Conservation*, in: Restauratorenblätter, Sonderband – Lacona I, Laser in the Conservation of Artworks, E. König, W. Kautek (ed.), Verlag Mayer & Comp., Vienna, 1997, pp. 57-60.

7. R. Bordalo, P. J. Morais, H. Gouveia, C. Young, *Laser Cleaning of Easel Paintings: An Overview*, Las. Chem., 2006, Article ID 90279.

8. V. Zafiropulos, T. Stratoudaki, A. Manousaki, K. Melesanaki, G. Orial, *Discoloration of pigments induced by laser irradiation*, Surf. Eng. 2001, **17**, 249-252.

9. M. Castillejo, M. Martin, M. Oujja, J. Santamaria, D. Silva, R. Torres, A. Manousaki, V. Zafiropulos, O.F. van den Brink, R.M.A. Heeren, R. Teule, A. Silva, *Evaluation of the chemical and physical changes induced by KrF laser irradiation of tempera paints*, J. Cult. Her., 2003, **4**, 257s–263s.

10. M. I. Cooper, *Laser Cleaning in Conservation: An Introduction*, in: Laser Cleaning in Conservation: an Introduction, M. Cooper (ed.), Butterworth-Heinemann, Oxford, 1998.

11. V. Zafiropulos, C. Fotakis, *Lasers in the conservation of painted artworks*, in: Laser Cleaning in Conservation: an Introduction, M. Cooper (ed.), Butterworth-Heinemann, Oxford, 1998.

12. C. Theodorakopoulos, *The excimer laser ablation of pictur evarnishes: an evaluation with reference to light-induced deterioration*, PhD Thesis, RCA/AMOLF, London, UK, 2005.

13. A. Athanassiou, A. E. Hill, T. Fourrier, L. Burgio, R.J.H. Clark, *The effects of UV laser light radiation on artists' pigments*, J. Cult. Her. 2000, **1**, S209-S213.

14. P. Pouli, D.C. Emmony, *The effect of Nd:YAG laser radiation on medieval pigments*, J. Cult. Her. 2000, **1**, S181–S188.

15. A. Sansonetti, M. Realini, *Nd:YAG laser effects on inorganic pigments*, J. Cult. Her. 2000, **1**, S189-S198.

16. A. Andreotti, P. Bracco, M. P. Colombini, A. deCruz, G. Lanterna, K. Nakahara, F. Penaglia, *Novel applications of the Er:YAG laser cleaning of old paintings*, in: Proceedings of the 6th International Conference on Lasers in the Conservation of Artworks (Lacona VI '05), J. Nimmrichter, W. Kautek, M. Schreiner (ed.), vol. 116 of Springer Proceedings in Physics, Vienna, Austria, 2005, pp. 269-279.

17. R. Bordalo, P. J. Morais, C. R. T. Young, L. F. Santos, R. M. Almeida, *The Effect of Excimer Laser Irradiation on Selected Pigments Used in the 19th Century*, ICOM-CC Triennial Meeting Lisbon, September 2011.

18. R. Bordalo, *Characterization of the Alterations Induced by UV Laser Radiation on the Pigmented Oil layers in Nineteenth Century Paintings on Canvas*, PhD thesis, Courtauld Institute of Art, University of London, 2011.